Letter

Observing altermagnetism using polarized neutrons

Paul A. McClarty,[1,*] Arsen Gukasov,[1,†] and Jeffrey G. Rau[2,‡]

[1]*Laboratoire Léon Brillouin, CEA, CNRS, Université Paris-Saclay, CEA-Saclay, 91191 Gif-sur-Yvette, France*

[2]*Department of Physics, University of Windsor, 401 Sunset Avenue, Windsor, Ontario N9B 3P4, Canada*

(Received 28 October 2024; accepted 21 January 2025; published 10 February 2025)

Altermagnets are collinear compensated magnets whose magnetic symmetries at zero spin-orbit coupling break spin degeneracy leading to spin-split electronic and magnonic bands that reflect an underlying multipolar order. When there is an approximate $U(1)$ symmetry the magnons in altermagnets are split into equal and opposite chiral pairs. We show that in altermagnets polarized neutrons provide a means to detect the population of time-reversed domains and allow direct measurement of the magnon chirality anisotropy in momentum space—the central signature of the altermagnetic phase. We demonstrate this response to polarized neutrons in two candidate materials MnF_2 and MnTe and show that the presence of these chiralities is stable to small perturbations that break spin-rotation symmetry. This provides a magnonic analog of spin-polarized ARPES that has been used to discern altermagnetism in the electronic band structures of various candidate materials.

DOI: 10.1103/PhysRevB.111.L060405

Many of the advances in condensed matter physics of this century have originated from a focus on systems with strong spin-orbit coupling. This has been true of much of the broader field of band topology as well as in research into exotic superconductivity and the collective phenomena of magnetic systems. In recent years there has been renewed interest in systems where the spin-orbit coupling is *weak* driven, in part, by the presence of generalized symmetries such as spin-space symmetries [1–7]. This is exemplified by the discovery of altermagnetism [8–10] where the conditions for spin degeneracy are broken in antiferromagnets at zero spin-orbit coupling as a direct consequence of their distinctive magnetocrystalline symmetries.

Altermagnets, as defined from the zero spin-orbit coupled limit, have the feature that their electronic bands are spin split and feature an anisotropy in momentum space [8–10] reflecting an underlying multipolar order [11,12]. Recently, ARPES and its spin-polarized analog have been used to directly visualize the breaking of spin degeneracy along momentum-space cuts in altermagnetic candidate materials such as MnTe [13,14].

Signatures of altermagnetism are also visible via the magnetic excitations [15,16]. In a classic Heisenberg-Néel antiferromagnet with two magnetic sublattices there is a single doubly degenerate magnon band due to a good quantum number defining a magnon "chirality" [17]. The existence of this conserved chirality is little more than a curiosity under these circumstances, with weak spin-orbit coupling often favoring states with zero net chirality. While in an antiferromagnet these chiralities can only be split using (e.g.) a magnetic field, in an altermagnet the magnon chiralities are intrinsically split in energy due to an isotropic exchange over most of the Brillouin zone—exhibiting the *same* anisotropy in momentum space as the one present in their electronic bands. Experimental evidence for this altermagnetic splitting has been observed in MnTe [18] and should be observable in MnF_2 through measurements along specific high-symmetry directions [1].

In this Letter, we point out that neutron scattering provides the means to distinguish all altermagnetic magnetic domains, including those related by time reversal, and the chiralities of the magnon modes in altermagnets. We show that this is a *general* feature of altermagnets—a direct consequence of their defining symmetries—and that it is stable to the inclusion of weak spin-orbit coupling. The key to these measurements is the ability to control the polarization of the ingoing neutron beam and to measure the polarization of the scattered beam. It is often said that altermagnets blend certain properties of ferromagnets and antiferromagnets. As we show, a majority single-domain altermagnet polarizes an initially unpolarized neutron beam through inelastic scattering from its magnon excitations. In this sense altermagnets behave like ferromagnets [19] despite being entirely compensated like antiferromagnets. However, the direction of polarization has a much richer dependence on the local moment orientation, magnon band, and scattering wave vector than in simple ferromagnets. Experiments using polarized neutrons can thus be used to map out the anisotropic splitting of chirality, just as spin-polarized ARPES can be used to map out the anisotropic pattern of spin splitting of the electronic band structures of altermagnets. Going further, the relative intensities of each of the chiral modes can be modulated across the Brillouin zone by tuning the polarization of the ingoing neutron beam. By taking data with flipped ingoing polarizations it is possible to isolate and measure the chiralities of the magnon bands individually, mirroring the signature in the outgoing polarization.

Observability of these effects rests on having a sample with an imbalance in the populations of domains related by time

*Contact author: paul.mcclarty@cea.fr
†Contact author: arsen.goukassov@cea.fr
‡Contact author: jrau@uwindsor.ca

reversal—ideally a single magnetic domain. In some systems this can be practically achieved by annealing from a high-field state (as has been done in MnF_2 [20,21]). We give a general argument that, in altermagnets, (elastic) neutron polarimetry can distinguish such domains thus providing the means to identify or validate suitable samples for inelastic scattering experiments using polarized neutrons. Whereas previous work has demonstrated experimentally that magnon chirality can be probed using polarized neutrons in uncompensated magnets [22,23], this work establishes neutron polarization as a powerful tool to characterize altermagnets generally through their magnetic excitations.

We organize the rest of the Letter as follows. We first explain how the ratio of time-reversed domains in altermagnets can be measured by exploiting nuclear-magnetic interference in neutron diffraction. We then give a brief introduction to altermagnetic splittings of chiral magnon modes including examples of toy models for candidate altermagnetic materials MnF_2 and MnTe. Turning then to inelastic neutron scattering of polarized neutrons, we show that the chiralities of altermagnetic magnons can be measured in the spin-orbit free limit. Finally, we discuss the role of spin-orbit coupling as a perturbation to this limit which is potentially an important consideration when carrying out studies of real altermagnetic materials.

Diffraction. The cross section for neutron diffraction using unpolarized neutrons is time-reversal invariant and therefore they cannot be used to distinguish magnetic domains related by time-reversal symmetry. However, when the neutrons are polarized, there is a contribution in the cross section that is time-reversal odd originating from the interference of nuclear and magnetic contributions. This contribution can, in principle, distinguish such magnetic domains.

This point was made already in 1962 [20] for the case of MnF_2. The observation in that work rests on the identification of the crystalline symmetries now central to defining altermagnetism. The generalization of their argument to all collinear centrosymmetric altermagnets is as follows.

For this discussion it will be sufficient to consider moments aligned or antialigned along a common axis $\hat{\boldsymbol{N}}$. Then the relevant contribution to the elastic cross section at a reciprocal lattice vector, $\boldsymbol{G}$, of the crystal lattice is proportional to

$$\propto (\hat{\boldsymbol{N}} \cdot \boldsymbol{P}_{\text{in}}^{\perp}) \text{Re}[F_{\text{nuc}}(\boldsymbol{G}) F_{\text{mag}}^{*}(\boldsymbol{G})]. \tag{1}$$

Here $\boldsymbol{P}_{\text{in}}^{\perp} \equiv \hat{\boldsymbol{G}} \times (\boldsymbol{P}_{\text{in}} \times \hat{\boldsymbol{G}})$ with $\boldsymbol{P}_{\text{in}}$ the polarization of the ingoing neutron beam. The contribution from the basis of sites in the primitive cell is $F_{\text{nuc}}(\boldsymbol{G}) = \sum_n \exp(i\boldsymbol{G} \cdot \boldsymbol{\delta}_n) b_n$ where b_n is the scattering length of the nth nucleus in the unit cell and $\boldsymbol{\delta}_n$ is its position. The magnetic contribution is similar with $F_{\text{mag}}(\boldsymbol{G}) = \sum_n \mu_n \sigma_n f_n(\boldsymbol{G}) \exp(i\boldsymbol{G} \cdot \boldsymbol{\delta}_n)$ where $\sigma_n = \pm 1$ specifies the moment direction of each magnetic atom with respect to $\hat{\boldsymbol{N}}$ and, μ_n, its size, while $f_n(\boldsymbol{G})$ is its magnetic form factor.

An altermagnet can be thought of as a colinear compensated magnet where the oppositely oriented magnetic sublattices *cannot* be connected by time reversal combined with either translation or inversion. Instead they are connected, for example, by the combined operations of translation, *rotation*, and time reversal. Consider first the conventional case, where the ions in the primitive cell can be grouped into two sets related by a translation $\boldsymbol{\tau}$ and time reversal. Then the magnetic part, containing only the magnetic ions, takes the form $F_{\text{mag}}^{*}(\boldsymbol{G}) = \Phi_{\text{mag}}(\boldsymbol{G})[1 - \exp(-i\boldsymbol{G} \cdot \boldsymbol{\tau})]$ where $\Phi_{\text{mag}}(\boldsymbol{G})$ is real. The nuclear contribution takes a similar form with $F_{\text{nuc}}(\boldsymbol{G}) = \Phi_{\text{nuc}}(\boldsymbol{G})[1 + \exp(i\boldsymbol{G} \cdot \boldsymbol{\tau})]$. The product has vanishing real part so the domains related by time reversal cannot be distinguished using polarized neutrons. Instead consider the case where there are two groups related by time reversal and inversion. Now $F_{\text{mag}}^{*}(\boldsymbol{G}) = \Phi_{\text{mag}}^{*}(\boldsymbol{G}) - \Phi_{\text{mag}}^{*}(-\boldsymbol{G})$ and $F_{\text{nuc}}(\boldsymbol{G}) = \Phi_{\text{nuc}}(\boldsymbol{G}) + \Phi_{\text{nuc}}(-\boldsymbol{G})$. As $\Phi_{\text{nuc}}(\boldsymbol{G})$ and $\Phi_{\text{mag}}(\boldsymbol{G})$ are sums of phases perhaps weighted with (real-valued) scattering lengths or moment lengths (etc.), for both $\Phi(\boldsymbol{G}) = \Phi^{*}(-\boldsymbol{G})$ and so, again, the real part vanishes.

To see that this part of the cross section can indeed be nonvanishing in an altermagnet we take the elementary example of MnF_2. This is tetragonal with primitive lattice vectors $\boldsymbol{a}_1 = a\hat{\boldsymbol{x}}$, $\boldsymbol{a}_2 = a\hat{\boldsymbol{y}}$, and $\boldsymbol{a}_3 = c\hat{\boldsymbol{z}}$. Using these basis vectors the magnetic ions lie at (0,0,0) and $(1/2, 1/2, 1/2)$ while the fluoride ions lie at $(\pm\epsilon, \pm\epsilon, 0)$ and $(1/2 \pm \epsilon, 1/2 \mp \epsilon, 1/2)$. The nuclear-magnetic contribution to the scattering intensity is then from Eq. (1),

$$\text{Re}[F_{\text{nuc}}(\boldsymbol{G}) F_{\text{mag}}^{*}(\boldsymbol{G})] \propto \mu \sin(aG_x\epsilon) \sin(aG_y\epsilon)[1 - \cos(\boldsymbol{G} \cdot \boldsymbol{\delta})].$$

The Bragg reflections for this lattice are indexed by $\boldsymbol{G} = 2\pi(G_1\hat{\boldsymbol{x}}/a + G_2\hat{\boldsymbol{y}}/b + G_3\hat{\boldsymbol{z}}/c)$ for $(G_1, G_2, G_3) \in \mathbb{Z}$. The nuclear-magnetic scattering is then nonvanishing for $G_1 + G_2 + G_3$ odd. Therefore, if we measure the Bragg intensities at these reflections $I_{\pm}$ for both flipped polarizations $\pm\boldsymbol{P}_{\text{in}}^{\perp}$ then a nonvanishing net polarization (asymmetry) $(I_+ - I_-)/(I_+ + I_-)$ signals the presence of one majority time-reversed domain.

As a second example, we consider altermagnetic candidate MnTe for which the Mn atoms are at positions $\boldsymbol{\delta}_{\text{Mn},1} = (0, 0, 0)$ and $\boldsymbol{\delta}_{\text{Mn},2} = (0, 0, 1/2)$ (with equal and opposite moments) and the Te atoms have positions $\boldsymbol{\delta}_{\text{Te},1} = (1/3, 2/3, 1/4)$ and $\boldsymbol{\delta}_{\text{Te},2} = (2/3, 1/3, 3/4)$ in terms of the usual hexagonal basis vectors ($\boldsymbol{a}_1 = a\hat{\boldsymbol{x}}$, $\boldsymbol{a}_2 = -a/2\hat{\boldsymbol{x}} + \sqrt{3}a/2\hat{\boldsymbol{y}}$, and $\boldsymbol{a}_3 = c\hat{\boldsymbol{z}}$). Now, one finds that

$$\text{Re}[F_{\text{nuc}}(\boldsymbol{G}) F_{\text{mag}}^{*}(\boldsymbol{G})] \propto \mu[\cos(\boldsymbol{G} \cdot \boldsymbol{\delta}_{\text{Te},1}) + \cos(\boldsymbol{G} \cdot \boldsymbol{\delta}_{\text{Te},2})],$$

when $\boldsymbol{G} \cdot \boldsymbol{b}_3 = G_3$ is odd and zero otherwise. Thus the nuclear-magnetic polarization dependent scattering at reflections with G_3 odd can distinguish the direction of the altermagnetic order.

Altermagnetic magnons. The peculiar symmetries of altermagnets described above in the zero spin-orbit limit have two central consequences. One is to preserve the spin quantum number of the electronic bands and the chirality of the magnon bands. The second, originating from the replacement of time-reversal symmetry by time reversal in conjunction with a point group operation, is to lift the degeneracy of the spins and chiralities in an anisotropic pattern in reciprocal space. In a d-wave altermagnet, for example, a fourfold rotation in momentum at fixed energy reverses both spins and magnon chiralities.

We can see how these features arise in a simple setting: a two-sublattice collinear compensated magnet with a

$U(1)$ symmetry along the moment direction $\hat{\boldsymbol{N}}$. The Holstein-Primakoff bosons on the two sublattices (labeled A and B) transform under this $U(1)$ symmetry as

$$a_{\boldsymbol{k},\mathrm{A}} \to e^{+i\theta} a_{\boldsymbol{k},\mathrm{A}}, \quad a_{\boldsymbol{k},\mathrm{B}} \to e^{-i\theta} a_{\boldsymbol{k},\mathrm{B}}.$$

At the level of linear spin waves, this restricts the Hamiltonian to have the form

$$H = \sum_{\boldsymbol{k}} \left[A^{\mathrm{A}}_{\boldsymbol{k}} a^{\dagger}_{\boldsymbol{k},\mathrm{A}} a_{\boldsymbol{k},\mathrm{A}} + A^{\mathrm{B}}_{\boldsymbol{k}} a^{\dagger}_{\boldsymbol{k},\mathrm{B}} a_{\boldsymbol{k},\mathrm{B}} + \left(B^{\mathrm{AB}}_{\boldsymbol{k}} a^{\dagger}_{\boldsymbol{k},\mathrm{A}} a^{\dagger}_{-\boldsymbol{k},\mathrm{B}} + \mathrm{H.c.} \right) \right].$$

It is natural to write $A^{\mathrm{A}}_{\boldsymbol{k}}$ and $A^{\mathrm{B}}_{\boldsymbol{k}}$ equivalently as $A^{\mathrm{A}}_{\boldsymbol{k}} = A_{\boldsymbol{k}} + \delta A_{\boldsymbol{k}}/2$ and $A^{\mathrm{B}}_{\boldsymbol{k}} = A_{\boldsymbol{k}} - \delta A_{\boldsymbol{k}}/2$ as well as defining $B^{\mathrm{AB}}_{\boldsymbol{k}} = B^{\mathrm{BA}}_{-\boldsymbol{k}} \equiv B_{\boldsymbol{k}}$. If we further assume an inversion symmetry, as is present in many of the canonical examples of altermagnets, then $A_{\boldsymbol{k}} = A_{-\boldsymbol{k}}$ and $B^{*}_{\boldsymbol{k}} = B_{-\boldsymbol{k}} = B_{\boldsymbol{k}}$. The relevant Bogoliubov matrix is then [17,24]

$$\boldsymbol{M}_{\boldsymbol{k}} = \begin{pmatrix} A_{\boldsymbol{k}} + \frac{1}{2}\delta A_{\boldsymbol{k}} & 0 & 0 & B_{\boldsymbol{k}} \\ 0 & A_{\boldsymbol{k}} - \frac{1}{2}\delta A_{\boldsymbol{k}} & B_{\boldsymbol{k}} & 0 \\ 0 & B_{\boldsymbol{k}} & A_{\boldsymbol{k}} + \frac{1}{2}\delta A_{\boldsymbol{k}} & 0 \\ B_{\boldsymbol{k}} & 0 & 0 & A_{\boldsymbol{k}} - \frac{1}{2}\delta A_{\boldsymbol{k}} \end{pmatrix}.$$

Due to the $U(1)$ symmetry, the diagonalization of these two independent blocks yields the spin-wave energies

$$\epsilon_{\boldsymbol{k},1} = +\tfrac{1}{2}\delta A_{\boldsymbol{k}} + \sqrt{A^2_{\boldsymbol{k}} - B^2_{\boldsymbol{k}}} \equiv \Omega_{\boldsymbol{k}} + \tfrac{1}{2}\delta A_{\boldsymbol{k}}, \tag{2a}$$

$$\epsilon_{\boldsymbol{k},2} = -\tfrac{1}{2}\delta A_{\boldsymbol{k}} + \sqrt{A^2_{\boldsymbol{k}} - B^2_{\boldsymbol{k}}} \equiv \Omega_{\boldsymbol{k}} - \tfrac{1}{2}\delta A_{\boldsymbol{k}}. \tag{2b}$$

The splitting of the two magnon bands is thus given by $|\epsilon_{\boldsymbol{k},1} - \epsilon_{\boldsymbol{k},2}| = |\delta A_{\boldsymbol{k}}|$ and thus vanishes when symmetry requires $A^{\mathrm{A}}_{\boldsymbol{k}} = A^{\mathrm{B}}_{\boldsymbol{k}}$. In an altermagnet there is no such symmetry—the operations linking the sublattices involve a spatial operation—and thus $\delta A_{\boldsymbol{k}}$ is generally nonzero. If this symmetry operation is denoted as R, then this implies $\delta A_{R(\boldsymbol{k})} = -\delta A_{\boldsymbol{k}}$, following the same anisotropy present in the spin splitting as the electronic bands.

Importantly, the associated eigenvectors are not affected by $\delta A_{\boldsymbol{k}}$, since its contribution is proportional to the identity in each Bogoliubov subblock. The eigenvectors associated with each positive energy mode can thus be written as

$$u_{\boldsymbol{k}} = \sqrt{\frac{\Omega_{\boldsymbol{k}} + A_{\boldsymbol{k}}}{2\Omega_{\boldsymbol{k}}}}, \quad v_{\boldsymbol{k}} = -\frac{B_{\boldsymbol{k}}}{\sqrt{2\Omega_{\boldsymbol{k}}(\Omega_{\boldsymbol{k}} + A_{\boldsymbol{k}})}}, \tag{3}$$

which satisfy $|u_{\boldsymbol{k}}|^2 - |v_{\boldsymbol{k}}|^2 = 1$. The standard (unpolarized) neutron dynamical structure factor can be expressed in terms of these quantities. The (textbook) result is that one-magnon intensity [17] is $\propto [1 + (\hat{\boldsymbol{N}} \cdot \hat{\boldsymbol{k}})^2] C_{\boldsymbol{k}}$ where

$$C_{\boldsymbol{k}} = \sqrt{\frac{A_{\boldsymbol{k}} + B_{\boldsymbol{k}}}{A_{\boldsymbol{k}} - B_{\boldsymbol{k}}}}. \tag{4}$$

The intensities of these two chiral modes are thus identical when ignoring neutron polarization, even when a nonzero altermagnetic splitting is present.

We now take an explicit example: that of insulating MnF_2. As Mn^{2+} has quenched orbital angular momentum $L = 0$ and spin $S = 5/2$ we expect the principal magnetic couplings to be highly isotropic. A minimal model for the altermagnetism in this material could include nearest-neighbor exchange with a coupling J between the two magnetic sublattices. With this coupling alone, the modes are doubly degenerate, with $\epsilon_{\boldsymbol{k},1} = \epsilon_{\boldsymbol{k},2} = 8JS(1 - \gamma^2_{\boldsymbol{k}})^{1/2}$ and $C_{\boldsymbol{k}} = [(1 - \gamma_{\boldsymbol{k}})/(1 + \gamma_{\boldsymbol{k}})]^{1/2}$ where $\gamma_{\boldsymbol{k}} = \cos(ak_x/2)\cos(ak_y/2)\cos(ck_z/2)$. This (accidental) degeneracy originates from the fact that the nearest-neighbor coupling has a higher symmetry than the lattice [16,25]. The shortest-range exchange that has the true symmetry of the lattice appears with representative bond direction along $a(\hat{\boldsymbol{x}} + \hat{\boldsymbol{y}})$. At this distance there are two inequivalent couplings J_{110} and J'_{110} which, when different, induce a finite $\delta A_{\boldsymbol{k}}$ lifting the degeneracy of the two magnon bands. Explicitly one finds that

$$A_{\boldsymbol{k}} = 8SJ + 2S(J_{110} + J'_{110})[\cos(ak_x)\cos(ak_y) - 1], \tag{5a}$$

$$\delta A_{\boldsymbol{k}} = 4S(J_{110} - J'_{110})\sin(ak_x)\sin(ak_y), \tag{5b}$$

$$B_{\boldsymbol{k}} = -8SJ\gamma_{\boldsymbol{k}}. \tag{5c}$$

The degeneracy of the modes is therefore lifted over much of the zone except in the $[h0l]$ and $[0kl]$ planes and at the zone boundaries where $\delta A_{\boldsymbol{k}}$ vanishes. Note that $\delta A_{\boldsymbol{k}}$ changes sign between the quadrants $k_x k_y > 0$ and $k_x k_y < 0$ reversing the chirality of the modes at a given energy. This is the magnonic signature of a d-wave altermagnet. An illustration of these magnon bands (and their chirality) is shown in Fig. 1(a).

A similar exercise can be carried out for the MnTe magnetic structure which is a g-wave altermagnet. As before, we couple the different magnetic sublattices via Heisenberg exchange to nearest neighbor. Then we include the shortest-range couplings that break the symmetry down to that of the lattice. Reference [25] contains a systematic study of the couplings that generate altermagnetism from which we read off the J_{121} exchanges along the representative bond $\boldsymbol{r}_1 \equiv (1, 2, 1)$ with threefold symmetry and inversion giving six bonds $\pm\boldsymbol{r}_1$, $\pm\boldsymbol{r}_2$, $\pm\boldsymbol{r}_3$ with the same coupling. There is a second symmetry-inequivalent coupling J'_{121} with the same bond length as the J_{121} bond but with representative $\boldsymbol{r}'_1 \equiv (1, 2, -1)$ and six equivalent bonds $\pm\boldsymbol{r}'_1$, $\pm\boldsymbol{r}'_2$, $\pm\boldsymbol{r}'_3$ under symmetry. Defining $\gamma_{\boldsymbol{k}} \equiv \sum_{\mu=1}^{3} \cos(\boldsymbol{k} \cdot \boldsymbol{r}_\mu)$ and $\gamma'_{\boldsymbol{k}} \equiv \sum_{\mu=1}^{3} \cos(\boldsymbol{k} \cdot \boldsymbol{r}'_\mu)$ one finds

$$A_{\boldsymbol{k}} = 2SJ + S(J_{121} + J'_{121})(\gamma_{\boldsymbol{k}} + \gamma'_{\boldsymbol{k}} - 6), \tag{6a}$$

$$\delta A_{\boldsymbol{k}} = 2S(J_{121} - J'_{121})(\gamma_{\boldsymbol{k}} - \gamma'_{\boldsymbol{k}}), \tag{6b}$$

$$B_{\boldsymbol{k}} = 2SJ\cos(ck_z/2), \tag{6c}$$

as the role of J_{121} and J'_{121} swap in going from sublattice A to sublattice B. This has degeneracies at $[hk0]$, the planes $[h0l]$, and at the zone boundaries where $\delta A_{\boldsymbol{k}} = 0$. The chiralities reverse in the upper (lower) energy band under a sixfold rotation so the model exhibits g-wave altermagnetism in the magnon bands. The model of Liu *et al.* [18] includes other short-range exchanges (e.g., J_2, J_3); while we have neglected these in Eq. (6a) for simplicity they are included in the explicit calculations shown in Fig. 2.

While we have focused on the case of two magnetic sublattices where the magnons are theoretically simple, the chirality remains well defined whenever there is a global $U(1)$ symmetry. This thus still leads to positive and negative chirality blocks in the linear spin wave Hamiltonian. Altermagnetism in such bipartite crystal structures with more than two

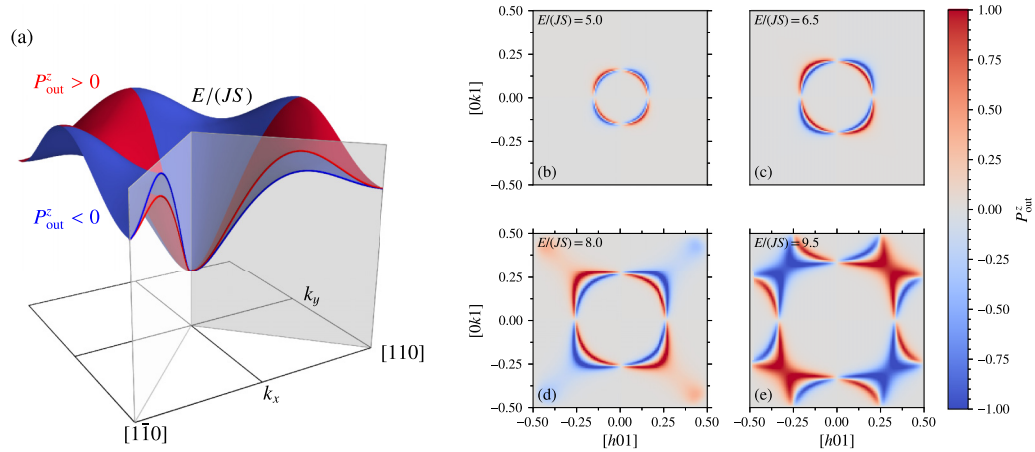

FIG. 1. (a) Illustration of the magnon dispersion of MnF_2 ($J_{110}/J = -0.25, J'_{110}/J = -0.5$) with finite altermagnetic exchange differences in the $[h, k, 0.25]$ plane. The order parameter is oriented along $\hat{z}$. The chirality of the magnon bands, which determines the polarization of outgoing neutrons $P^z_{\rm out}$, is indicated by the color of the bands. (b)–(e) Cuts in the $[hk1]$ plane at fixed energy $E/(JS)$ of the dispersion of the MnF_2 magnon bands showing the polarization of the outgoing neutron at each energy and wave vector [see Eq. (8)]. Polarization is averaged with a (Lorentzian) energy broadening $\delta E/JS = 0.25$ to loosely mimic finite experimental resolution.

sublattices thus should be detectable using polarized neutrons in a similar manner.

Detecting polarized altermagnetic magnons. We have seen that while unpolarized neutrons can detect the altermagnetic splitting in the energy bands, they are not sensitive to the polarization of the modes. However, as was the case for domains in the elastic scattering, the chirality of these altermagnetic magnons *can* be detected using polarized neutrons. We will describe two complementary experimental setups to observe this polarization.

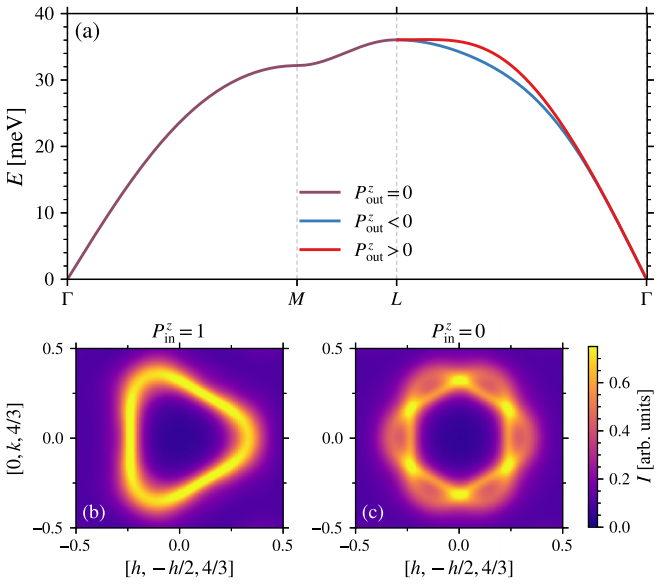

FIG. 2. (a) Magnon dispersion of MnTe using the parameters from Liu *et al.* [18] along a path Γ-M-L-Γ in momentum space [see Eq. (6a)]. The chirality of the magnon bands, which determines the polarization of outgoing neutrons $P^z_{\rm out}$, is indicated by the color of the bands and is visible along the Γ-L line, canceling due to symmetry along the other segments of the path. (b), (c) Comparison of neutron scattering intensity in the k_x-k_y plane with $k_z = 4/3(2\pi/c)$ at $E = 33$ meV for polarized ($P^z_{\rm in} = 1$) and unpolarized ($P^z_{\rm in} = 0$) incoming neutrons [see Eq. (7)]. Intensity is averaged with a (Lorentzian) energy broadening $\delta E = 1$ meV to loosely mimic finite experimental resolution.

First one can consider the total scattering intensity of an initial polarized beam with initial polarization $\boldsymbol{P}_{\rm in}$ [17,26],

$$\left(\frac{d^2\sigma}{d\Omega d\omega}\right) \propto \int dt e^{-i\omega t}[\langle \boldsymbol{M}^{\perp}_{-\boldsymbol{k}} \cdot \boldsymbol{M}^{\perp}_{\boldsymbol{k}}(t)\rangle + i\boldsymbol{P}_{\rm in} \cdot \langle \boldsymbol{M}^{\perp}_{-\boldsymbol{k}} \times \boldsymbol{M}^{\perp}_{\boldsymbol{k}}(t)\rangle], \quad (7)$$

where we have defined $\boldsymbol{M}^{\perp}_{\boldsymbol{k}} \equiv \hat{\boldsymbol{k}} \times (\boldsymbol{M}_{\boldsymbol{k}} \times \hat{\boldsymbol{k}})$ with $\boldsymbol{M}_{\boldsymbol{k}} \equiv \sum_{\boldsymbol{r},n} \mu_n f_n(\boldsymbol{k}) e^{i\boldsymbol{k}\cdot(\boldsymbol{r}+\delta_n)} \boldsymbol{S}_{\boldsymbol{r},n}$ being the magnetization operator at wave vector $\boldsymbol{k}$ (assuming isotropic g factors). The polarization-dependent part couples to an antisymmetric combination of the moment operators and thus allows access to the antisymmetric components of the dynamical structure factor [27].

Alternatively, an initially unpolarized beam will become polarized by scattering from the altermagnetic magnons with the outgoing polarization $\boldsymbol{P}_{\rm out}$ given by

$$\boldsymbol{P}_{\rm out} = \left(\frac{d^2\sigma}{d\Omega d\omega}\right)^{-1}_{\boldsymbol{P}_{\rm in}=0} \int dt e^{-i\omega t}[-i\langle \boldsymbol{M}^{\perp}_{-\boldsymbol{k}} \times \boldsymbol{M}^{\perp}_{\boldsymbol{k}}(t)\rangle]. \quad (8)$$

This probes the *same* antisymmetric part of the dynamical structure that is accessible using the initially polarized beam.

Both of these quantities can be readily computed via spin-wave theory. The total intensity due to a polarized beam at zero temperature can be written in terms of weights associated with each magnon band as

$$\left(\frac{d^2\sigma}{d\Omega d\omega}\right) \propto \sum_n \mathcal{W}_{\boldsymbol{k},n}(\boldsymbol{P}_{\rm in})\delta(\omega - \epsilon_{\boldsymbol{k},n}).$$

The weights $\mathcal{W}_{\boldsymbol{k},n}(\boldsymbol{P}_{\rm in})$ are defined as

$$\mathcal{W}_{\boldsymbol{k},n}(\boldsymbol{P}_{\rm in}) = |\mathcal{A}^{\perp}_{\boldsymbol{k},n}|^2 + i\boldsymbol{P}_{\rm in} \cdot (\mathcal{A}^{\perp}_{\boldsymbol{k},n} \times [\mathcal{A}^{\perp}_{\boldsymbol{k},n}]^*),$$

in terms of $\mathcal{A}^{\perp}_{\boldsymbol{k},n} = \hat{\boldsymbol{k}} \times (\mathcal{A}_{\boldsymbol{k},n} \times \hat{\boldsymbol{k}})$, and where

$$\mathcal{A}^{\mu}_{\boldsymbol{k},n} \equiv \sum_m \left(\hat{e}^{\mu}_{m,-} V^m_{\boldsymbol{k},n,+} + \hat{e}^{\mu}_{m,+} V^m_{\boldsymbol{k},n,-}\right),$$

where m here runs over the magnetic atoms. Here we have split our Bogoliubov eigenvectors [28] into blocks as $\boldsymbol{V}^{\intercal}_{\boldsymbol{k},n} \equiv (\boldsymbol{V}^{\intercal}_{\boldsymbol{k},n,+}, \boldsymbol{V}^{\intercal}_{\boldsymbol{k},n,-})$ and denoted choice of Cartesian frame $\hat{\boldsymbol{e}}_{n,\pm} \equiv (\hat{\boldsymbol{x}}_n \pm i\hat{\boldsymbol{y}}_n)/\sqrt{2}$ for the nth magnetic ion. For the simple two-sublattice case discussed above, these vectors would be $\boldsymbol{V}^{\intercal}_{\boldsymbol{k},1} = (u_{\boldsymbol{k}}, 0, 0, v_{\boldsymbol{k}})$ and $\boldsymbol{V}^{\intercal}_{\boldsymbol{k},2} = (0, u_{\boldsymbol{k}}, v_{\boldsymbol{k}}, 0)$. Similarly we can express the polarization of the outgoing intensity at each of the magnon bands due to an initially unpolarized beam as

$$\boldsymbol{P}_{\text{out}}(\boldsymbol{k}, \epsilon_{\boldsymbol{k},n}) = -i \frac{\mathcal{A}^{\perp}_{\boldsymbol{k},n} \times [\mathcal{A}^{\perp}_{\boldsymbol{k},n}]^*}{\mathcal{A}^{\perp}_{\boldsymbol{k},n} \cdot [\mathcal{A}^{\perp}_{\boldsymbol{k},n}]^*}.$$

For the case of a collinear altermagnet with two sublattices and isotropic interactions, one can show that

$$-i\mathcal{A}^{\perp}_{\boldsymbol{k},n} \times [\mathcal{A}^{\perp}_{\boldsymbol{k},n}]^* = -(-1)^n \hat{\boldsymbol{k}}(\hat{\boldsymbol{k}} \cdot \hat{\boldsymbol{N}}) C_{\boldsymbol{k}},$$
$$\mathcal{A}^{\perp}_{\boldsymbol{k},n} \cdot [\mathcal{A}^{\perp}_{\boldsymbol{k},n}]^* = \tfrac{1}{2}[1 + (\hat{\boldsymbol{k}} \cdot \hat{\boldsymbol{N}})^2] C_{\boldsymbol{k}},$$

where $C_{\boldsymbol{k}}$ is the one-magnon intensity defined in Eq. (4). From these expressions we see that for an initially polarized beam the outgoing intensity is modulated by the polarization oppositely for the two bands

$$\mathcal{W}_{\boldsymbol{k},n}(\boldsymbol{P}_{\text{in}}) = \left(\tfrac{1}{2}[1 + (\hat{\boldsymbol{k}} \cdot \hat{\boldsymbol{N}})^2] + (-1)^n (\boldsymbol{P}_{\text{in}} \cdot \hat{\boldsymbol{k}})(\hat{\boldsymbol{k}} \cdot \hat{\boldsymbol{N}})\right) C_{\boldsymbol{k}}.$$

One may carry out such an experiment on an instrument in which the incident (or scattered) neutron beam is polarized using the method often referred to as the "half-polarized" or the "flipping-ratio" method. One gains the most insight by aligning the neutron polarization along the moment direction with $\boldsymbol{P}_{\text{in}} = \pm\hat{\boldsymbol{N}}$. One measures the cross section for $\boldsymbol{P}_{\text{in}} = +\hat{\boldsymbol{N}}$ and again for $-\hat{\boldsymbol{N}}$ and this gives access to the relevant terms. No polarization analysis is needed in this case; explicitly, if we define $\Delta\mathcal{W}_{\boldsymbol{k},n} \equiv [\mathcal{W}_{\boldsymbol{k},n}(+\hat{\boldsymbol{N}}) - \mathcal{W}_{\boldsymbol{k},n}(-\hat{\boldsymbol{N}})]/2$ and divide out the unpolarized result one directly arrives at

$$\frac{\Delta\mathcal{W}_{\boldsymbol{k},n}}{\mathcal{W}_{\boldsymbol{k},n}(\boldsymbol{0})} = (-1)^n \left(\frac{2(\hat{\boldsymbol{k}} \cdot \hat{\boldsymbol{N}})^2}{1 + (\hat{\boldsymbol{k}} \cdot \hat{\boldsymbol{N}})^2}\right),$$

independent of the one-magnon intensity factor $C_{\boldsymbol{k}}$.

The differing signs for the two modes directly correspond to their respective chiralities. Note that in situations where there is altermagnetic splitting for scattering wave vectors along the moment direction (which is certainly the case for ideal altermagnets), the entire scattering intensity for such wave vectors can be reweighted from one mode to the other simply by reversing the polarization direction of the ingoing beam.

Similarly for an initially unpolarized beam the polarization of the intensity of the magnon bands is opposite on each band,

$$\boldsymbol{P}_{\text{out}}(\boldsymbol{k}, \epsilon_{\boldsymbol{k},n}) = -(-1)^n \left(\frac{2(\hat{\boldsymbol{k}} \cdot \hat{\boldsymbol{N}})}{1 + (\hat{\boldsymbol{k}} \cdot \hat{\boldsymbol{N}})^2}\right) \hat{\boldsymbol{k}}.$$

For the component of the polarization along $\hat{\boldsymbol{N}}$ this yields the same result (up to sign) as $\Delta\mathcal{W}_{\boldsymbol{k},n}/\mathcal{W}_{\boldsymbol{k},n}(\boldsymbol{0})$. In this case, the experiments require use of a neutron polarization analyzer (for example, CRYOPAD [29,30]).

Examples of what experimental neutron scattering intensities might look like are shown in Figs. 1 and 2. For MnF_2 (Fig. 1) we show the outgoing polarization of the intensity for an initially unpolarized neutron beam. The polarization directly shows the d-wave symmetry of the magnon chirality in both the dispersion and fixed energy cuts. For MnTe (Fig. 2) we show the dispersion (with magnon chiralities indicated) and the neutron intensity for an experiment where the incoming neutrons are polarized. Compared to the unpolarized intensity, the polarization enhances the intensity of one chiral band, extinguishing the other and thus revealing the spatial g-wave structure of the magnon wave functions. For a smaller altermagnetic splitting (or broader energy resolution) this extinguishment will not be perfect, but a spatial anisotropy in the intensity should still be visible.

Weakly breaking the $U(1)$ symmetry. So far we have considered only ideal altermagnets where there is a residual $U(1)$ symmetry in the magnetically ordered state resulting in magnon modes with well-defined chirality. In altermagnetic materials, this symmetry is expected to hold to an excellent approximation. Weak anisotropic couplings will inevitably break this $U(1)$ down to the crystalline symmetries via (e.g.) the magnetostatic dipolar interaction or spin-orbit coupling. How does this affect chirality as a signature of altermagnetic magnons?

Start in the limit where the magnons are chiral and degenerate—for example in a conventional Heisenberg antiferromagnet or in an altermagnet at wave vectors where the degeneracy is protected by spin-space symmetries—and thus $\delta A_{\boldsymbol{k}} = 0$. Anisotropies breaking the $U(1)$ symmetry modify the spin wave Hamiltonian through the addition of a $\delta\boldsymbol{M}_{\boldsymbol{k}}$ of the form

$$\delta\boldsymbol{M}_{\boldsymbol{k}} = \begin{pmatrix} 0 & A^{\text{AB}}_{\boldsymbol{k}} & B^{\text{AA}}_{\boldsymbol{k}} & 0 \\ [A^{\text{AB}}_{\boldsymbol{k}}]^* & 0 & 0 & B^{\text{BB}}_{\boldsymbol{k}} \\ [B^{\text{AA}}_{\boldsymbol{k}}]^* & 0 & 0 & [A^{\text{AB}}_{\boldsymbol{k}}]^* \\ 0 & [B^{\text{BB}}_{\boldsymbol{k}}]^* & A^{\text{AB}}_{\boldsymbol{k}} & 0 \end{pmatrix}.$$

We assume that the perturbation is non-altermagnetic in the sense that it does not distinguish between the two sublattices and thus does not contribute to $\delta A_{\boldsymbol{k}}$ [31]. Any (perturbative) changes to $A_{\boldsymbol{k}}$, $B_{\boldsymbol{k}}$ will be absorbed into their definitions.

Projecting $\delta\boldsymbol{M}_{\boldsymbol{k}}$ into the subspace spanned by the eigenvectors $\boldsymbol{V}_{\boldsymbol{k},1}$ and $\boldsymbol{V}_{\boldsymbol{k},2}$ we obtain the effective Hamiltonian

$$\begin{pmatrix} 0 & t_{\text{eff}} \\ t^*_{\text{eff}} & 0 \end{pmatrix},$$

where we have defined $t_{\text{eff}} \equiv \boldsymbol{V}^{\dagger}_{\boldsymbol{k},1} \delta\boldsymbol{M}_{\boldsymbol{k}} \boldsymbol{V}_{\boldsymbol{k},2}$. The corrected eigenvectors are linear combinations of $\boldsymbol{V}_{\boldsymbol{k},1}$ and $\boldsymbol{V}_{\boldsymbol{k},2}$ of the form

$$\frac{1}{\sqrt{2}}(\boldsymbol{V}_{\boldsymbol{k},1} \pm e^{-i\phi} \boldsymbol{V}_{\boldsymbol{k},2}),$$

where $t_{\text{eff}} \equiv |t_{\text{eff}}| e^{i\phi}$. Correspondingly we have the new $\mathcal{A}_{\boldsymbol{k},\pm}$ and the the polarization-dependent contribution is then proportional to

$$i\mathcal{A}^{\perp}_{\boldsymbol{k},\pm} \times [\mathcal{A}^{\perp}_{\boldsymbol{k},\pm}]^* = \pm\tfrac{1}{2}(ie^{-i\phi} \mathcal{A}^{\perp}_{\boldsymbol{k},2} \times [\mathcal{A}^{\perp}_{\boldsymbol{k},1}]^* - \text{c.c.}),$$

since $\mathcal{A}_{\boldsymbol{k},1} \times [\mathcal{A}^{\perp}_{\boldsymbol{k},1}]^* = -\mathcal{A}_{\boldsymbol{k},2} \times [\mathcal{A}^{\perp}_{\boldsymbol{k},2}]^*$. Then since we have $\mathcal{A}_{\boldsymbol{k},1} \propto [\mathcal{A}^{\perp}_{\boldsymbol{k},2}]^*$ their cross product vanishes. Thus small $U(1)$-breaking anisotropies, absent a finite $\delta A_{\boldsymbol{k}}$, tend to maximally mix the chiral modes leading to a vanishing polarization-dependent part of the neutron scattering cross section.

When both $U(1)$-breaking terms and $\delta A_{\boldsymbol{k}}$ are finite but small, the perturbative analysis follows standard first-order degenerate perturbation theory leading to an avoided crossing with splittings $\delta\epsilon_{\boldsymbol{k},\pm} = \pm\, 2[h^2_{\text{eff}} + |t_{\text{eff}}|^2]^{1/2}$ where $h_{\text{eff}} \propto \delta A_{\boldsymbol{k}}$. The polarization of each mode is then given by $\pm h_{\text{eff}}/[h^2_{\text{eff}} + |t_{\text{eff}}|^2]^{1/2}$, vanishing when $h_{\text{eff}} = 0$ and equal to ± 1 when $t_{\text{eff}} = 0$. For small t_{eff} we have polarizations $\pm(1 - |t_{\text{eff}}|^2/h_{\text{eff}} + \cdots)$ and thus the neutron polarization signatures discussed in this work are perturbatively stable.

Conclusions. We have shown that polarized neutron scattering has attractive features for the detection and characterization of altermagnets. In particular, elastic scattering with polarization analysis can be used to infer the domain composition of altermagnets. In samples that have been established to have a majority domain, we have described how polarized inelastic neutron scattering can provide a direct, unambiguous experimental signature of the altermagnetic chirality splitting of magnons. This could be used, for example, to reveal the g-wave altermagnetism in MnTe. While we have focused on local moment models of altermagnetism, we expect identical polarization signatures from magnon scattering in itinerant altermagnets. Potential future applications of such tools could be in probing features arising from magnon-magnon or magnon-electron interactions in altermagnets [32–34] through their polarization response. Insights from polarized neutrons can thus pave the way for the clear confirmation of altermagnetism in candidate materials and promise to become a central tool in this emerging field.

Note added. Recently, Ref. [35] appeared, reporting new unpolarized inelastic neutron scattering results on MnF_2 that probe the non-high-symmetry directions where altermagnetic splittings are allowed to appear. No resolvable splitting was observed, in contrast to MnTe. This null result likely indicates that the scale of the altermagnetic splitting, dictated by $J_{110} - J'_{110}$, is below the resolution of the CAMEA instrument (at PSI), which is roughly 0.4 meV at an energy transfer of 6.9 meV.

Acknowledgments. P.A.M. acknowledges financial support from the CNRS and useful discussions with Dalila Bounoua, Philippe Bourges, Françoise Damay, Quentin Faure, and Sylvain Petit. Work at the University of Windsor (J.G.R.) was funded by the Natural Sciences and Engineering Research Council of Canada (NSERC) (Funding Reference No. RGPIN-2020-04970).

[1] A. Corticelli, R. Moessner, and P. A. McClarty, Spin-space groups and magnon band topology, Phys. Rev. B **105**, 064430 (2022).

[2] P. Liu, J. Li, J. Han, X. Wan, and Q. Liu, Spin-group symmetry in magnetic materials with negligible spin-orbit coupling, Phys. Rev. X **12**, 021016 (2022).

[3] H. Schiff, A. Corticelli, A. Guerreiro, J. Romhányi, and P. McClarty, The spin point groups and their representations, arXiv:2307.12784.

[4] J. Yang, Z.-X. Liu, and C. Fang, Symmetry invariants in magnetically ordered systems having weak spin-orbit coupling, Nat. Commun. **15**, 10203 (2024).

[5] X. Chen, J. Ren, Y. Zhu, Y. Yu, A. Zhang, P. Liu, J. Li, Y. Liu, C. Li, and Q. Liu, Enumeration and representation theory of spin space groups, Phys. Rev. X **14**, 031038 (2024).

[6] Z. Xiao, J. Zhao, Y. Li, R. Shindou, and Z.-D. Song, Spin space groups: Full classification and applications, Phys. Rev. X **14**, 031037 (2024).

[7] Y. Jiang, Z. Song, T. Zhu, Z. Fang, H. Weng, Z.-X. Liu, J. Yang, and C. Fang, Enumeration of spin-space groups: Toward a complete description of symmetries of magnetic orders, Phys. Rev. X **14**, 031039 (2024).

[8] L. Šmejkal, R. González-Hernández, T. Jungwirth, and J. Sinova, Crystal time-reversal symmetry breaking and spontaneous Hall effect in collinear antiferromagnets, Sci. Adv. **6**, eaaz8809 (2020).

[9] S. Hayami, Y. Yanagi, and H. Kusunose, Momentum-dependent spin splitting by collinear antiferromagnetic ordering, J. Phys. Soc. Jpn. **88**, 123702 (2019).

[10] L. Šmejkal, J. Sinova, and T. Jungwirth, Emerging research landscape of altermagnetism, Phys. Rev. X **12**, 040501 (2022).

[11] P. A. McClarty and J. G. Rau, Landau theory of altermagnetism, Phys. Rev. Lett. **132**, 176702 (2024).

[12] S. Bhowal and N. A. Spaldin, Ferroically ordered magnetic octupoles in d-wave altermagnets, Phys. Rev. X **14**, 011019 (2024).

[13] Suyoung Lee, Sangjae Lee, S. Lee, S. Jung, J. Jung, D. Kim, Y. Lee, B. Seok, J. Kim, B. G. Park, L. Šmejkal, C.-J. Kang, and C. Kim, Broken Kramers degeneracy in altermagnetic MnTe, Phys. Rev. Lett. **132**, 036702 (2024).

[14] J. Krempaský, L. Šmejkal, S. W. D'Souza, M. Hajlaoui, G. Springholz, K. Uhlířová, F. Alarab, P. C. Constantinou, V. Strocov, D. Usanov, W. R. Pudelko, R. González-Hernández, A. B. Hellenes, Z. Jansa, H. Reichlová, Z. Šobáň, R. D. Gonzalez Betancourt, P. Wadley, J. Sinova, D. Kriegner *et al.*, Altermagnetic lifting of Kramers spin degeneracy, Nature **626**, 517 (2024).

[15] L. Šmejkal, A. Marmodoro, K.-H. Ahn, R. González-Hernández, I. Turek, S. Mankovsky, H. Ebert, S. W. D'Souza, O. Šipr, J. Sinova, and T. Jungwirth, Chiral magnons in altermagnetic RuO_2, Phys. Rev. Lett. **131**, 256703 (2023).

[16] M. Gohlke, A. Corticelli, R. Moessner, P. A. McClarty, and A. Mook, Spurious symmetry enhancement in linear spin wave theory and interaction-induced topology in magnons, Phys. Rev. Lett. **131**, 186702 (2023).

[17] W. Marshall and S. Lovesey, *Theory of Thermal Neutron Scattering: The Use of Neutrons for the Investigation of Condensed Matter*, International Series of Monographs on Physics (Clarendon Press, Oxford, UK, 1971).

[18] Z. Liu, M. Ozeki, S. Asai, S. Itoh, and T. Masuda, Chiral split magnon in altermagnetic MnTe, Phys. Rev. Lett. **133**, 156702 (2024).

[19] J. S. Schwinger, On the magnetic scattering of neutrons, Phys. Rev. **51**, 544 (1937).

[20] H. A. Alperin, P. J. Brown, R. Nathans, and S. J. Pickart, Polarized neutron study of antiferromagnetic domains in MnF_2, Phys. Rev. Lett. **8**, 237 (1962).

[21] G. P. Felcher and R. Kleb, Antiferromagnetic domains and the spin-flop transition of MnF_2, Europhys. Lett. **36**, 455 (1996).

[22] Y. Nambu, J. Barker, Y. Okino, T. Kikkawa, Y. Shiomi, M. Enderle, T. Weber, B. Winn, M. Graves-Brook, J. M. Tranquada, T. Ziman, M. Fujita, G. E. W. Bauer, E. Saitoh, and K. Kakurai, Observation of magnon polarization, Phys. Rev. Lett. **125**, 027201 (2020).

[23] K. Jenni, S. Kunkemöller, W. Schmidt, P. Steffens, A. A. Nugroho, and M. Braden, Chirality of magnetic excitations in ferromagnetic $SrRuO_3$, Phys. Rev. B **105**, L180408 (2022).

[24] J.-P. Blaizot and G. Ripka, *Quantum Theory of Finite Systems* (MIT Press, Cambridge, MA, 1986).

[25] A. K. Dagnino, A. Corticelli, M. Gohlke, A. Mook, R. Moessner, and P. A. McClarty, The landscape of symmetry enhancement in tight-binding models, arXiv:2409.02999.

[26] R. M. Moon, T. Riste, and W. C. Koehler, Polarization analysis of thermal-neutron scattering, Phys. Rev. **181**, 920 (1969).

[27] Note that this second term vanishes if $\boldsymbol{P}_{\text{in}} \cdot \hat{\boldsymbol{k}} = 0$ since $\boldsymbol{M}^{\perp}_{\boldsymbol{k}}$ is orthogonal to $\hat{\boldsymbol{k}}$ and $\boldsymbol{M}^{\perp}_{-\boldsymbol{k}} \times \boldsymbol{M}^{\perp}_{\boldsymbol{k}} \propto \hat{\boldsymbol{k}}$. For this configuration, when we perform neutron polarization analysis after scattering, the spin-flip and non-spin-flip parts thus only contain information about the symmetric part of the dynamical structure factor.

[28] See Supplemental Material at http://link.aps.org/supplemental/10.1103/PhysRevB.111.L060405 for a brief review of the theory of polarized elastic and inelastic neutron scattering and linear spin-wave theory relevant for the main text.

[29] F. Tasset, P. J. Brown, and J. B. Forsyth, Determination of the absolute magnetic moment direction in Cr_2O_3 using generalized polarization analysis, J. Appl. Phys. **63**, 3606 (1988).

[30] F. Tasset, Zero field neutron polarimetry, Phys. B: Condens. Matter **156-157**, 627 (1989).

[31] We note that anisotropic interactions generally realize the symmetry of the lattice even at short range. If the dominant short-range interactions are from sublattice A to B then this can at best only generate a constant contribution to $\delta A_{\boldsymbol{k}}$; wave-vector dependence must originate from intra-sublattice couplings.

[32] F. Reyes-Osorio and B. K. Nikolic, Nonlocal damping of spin waves in a magnetic insulator induced by normal, heavy, or altermagnetic metallic overlayer: A Schwinger-Keldysh field theory approach, Phys. Rev. B **110**, 214432 (2024).

[33] F. Garcia-Gaitan, A. Kefayati, J. Q. Xiao, and B. K. Nikolic, Magnon spectrum of altermagnets beyond linear spin wave theory: Magnon-magnon interactions via time-dependent matrix product states versus atomistic spin dynamics, Phys. Rev. B **111**, L020407 (2025).

[34] A. T. Costa, J. C. G. Henriques, and J. Fernández-Rossier, Giant spatial anisotropy of magnon lifetime in altermagnets, arXiv:2405.12896.

[35] V. C. Morano, Z. Maesen, S. E. Nikitin, J. Lass, D. G. Mazzone, and O. Zaharko, Absence of altermagnetic magnon band splitting in MnF_2, arXiv:2412.03545.